

# Efficient Multi-Grained Knowledge Reuse for Class Incremental Segmentation

Zhihe Lu, *Member, IEEE*, Shuicheng Yan, *Fellow, IEEE*, Xinchao Wang, *Senior Member, IEEE*

arXiv:2306.02027v1 [cs.CV] 3 Jun 2023

**Abstract**—Class Incremental Semantic Segmentation (CISS) has been a trend recently due to its great significance in real-world applications. Although the existing CISS methods demonstrate remarkable performance, they either leverage the high-level knowledge (feature) only while neglecting the rich and diverse knowledge in the low-level features, leading to poor old knowledge preservation and weak new knowledge exploration; or use multi-level features for knowledge distillation by retraining a heavy backbone, which is computationally intensive. In this paper, we for the first time propose to efficiently reuse the multi-grained knowledge for CISS by fusing multi-level features with the frozen backbone and show a simple aggregation of varying-level features, *i.e.*, naïve feature pyramid, can boost the performance significantly. We further introduce a novel densely-interactive feature pyramid (DEFY) module that enhances the fusion of high- and low-level features by enabling their dense interaction. Specifically, DEFY establishes a per-pixel relationship between pairs of feature maps, allowing for multi-pair outputs to be aggregated. This results in improved semantic segmentation by leveraging the complementary information from multi-level features. We show that DEFY can be effortlessly integrated into three representative methods for performance enhancement. Our method yields a new state-of-the-art performance when combined with the current SOTA by notably averaged mIoU gains on two widely used benchmarks, *i.e.*, 2.5% on PASCAL VOC 2012 and 2.3% on ADE20K.

**Index Terms**—Class incremental segmentation, Knowledge distillation, Feature pyramid, Dense interaction.

## I. INTRODUCTION

Deep models have achieved great success on semantic segmentation [1]–[11] in a close-set fashion since 2015 [1], but those models inevitably faced catastrophic forgetting [12]–[14] – a problem that was first proposed in 1989, *i.e.*, a model tends to forget the old knowledge when required to learn the new in sequential learning. Solving this problem is crucial and practical, *e.g.*, a self-driving system is always needed to recognize new environments or traffic signs without forgetting the old concepts. Incremental learning [15]–[22] provides a solution for this problem by learning a model in a continuous data stream, in which the learned model needs to perform well on both old and new scenarios.

Incremental learning has been introduced to semantic segmentation since 2019 [24], but the historical works were specialized to classification problem, which are not suitable for class incremental semantic segmentation (CISS) due to its unique issue – *background shift* [25]. That is, the background

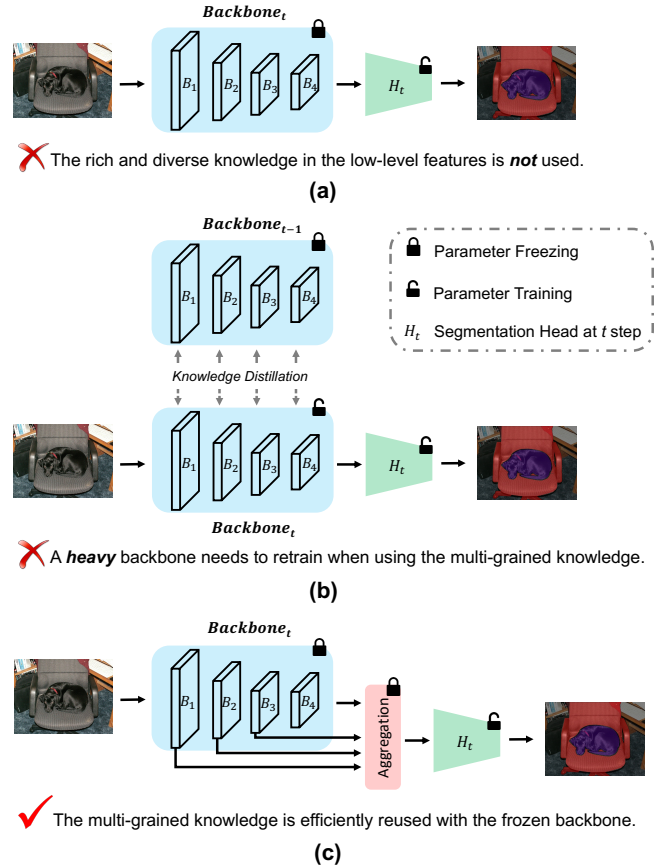


Fig. 1. Illustration of the difference between our method (c) and previous ones: (a) and (b). Obviously, our method is more advantageous by efficiently leveraging the multi-grained knowledge in varying-level features without retraining the heavy backbone.

in step  $t$  may contain not only current classes but also the past and future ones. Regarding *background shift*, two effective techniques have been proposed: old knowledge based pseudo labeling [23], [26], [27] and unknown class modeling [23], [27]. Specifically, the pseudo labeling combines the pseudo labels from the model of step  $t - 1$  and the ground-truth labels at step  $t$  to produce the updated labels containing both old and current classes, but it neglects the future classes that may exist in the background. This limitation can be tackled by unknown class modeling, which often utilizes a class-agnostic model [28], [29] to detect all objects in one image. These objects are then be used to model future classes. However, those methods encounter two limitations: (i) only the high-level knowledge (*the output of the feature extraction backbone*) is leveraged to

Manuscript received April 19, 2021; revised August 16, 2021.

Zhihe Lu (zhihelu.academic@gmail.com) and Xinchao Wang are with Learning and Vision Lab at National University of Singapore, Singapore

Shuicheng Yan is with BAAI, Beijing, China.

Corresponding author: Xinchao Wang, xinchao@nus.edu.sg.



Fig. 2. Illustrating the significance of using multi-grained knowledge for CISS. The top two rows are the results using the high-level knowledge (the feature  $f_4$ ) only while the bottom two show the results with multi-grained knowledge (four-level features  $f_1, f_2, f_3, f_4$ ) being used.  $f_i$ : the feature extracted from the  $i^{th}$  block of ResNet-101. With the high-level knowledge only, the model tends to not only forget the old knowledge learned in the first step, e.g., the “cow” is misclassified as “sheep” in the 1<sup>st</sup> row, but also lose the ability to learn new classes, e.g., the “TV” is totally missed (2<sup>nd</sup> row). In contrast, using multi-grained knowledge (bottom two) can enhance both old knowledge preservation and new knowledge exploration for CISS. Baseline: MicroSeg [23]. Set-up: **15-5 (2 steps)** on PASCAL VOC 2012.

perform pseudo labeling and unknown class modeling [23], [27] while the low-level features that also contain abundant prior knowledge as well as more detailed semantics [3] are not used as shown in Figure 1 (a), weakening its capability to preserve old knowledge and learn new classes (see the first two rows in Figure 2); and (ii) a heavy backbone, e.g., ResNet-101, is needed to retrain in the incremental step [26], [30] when reusing multi-level features for knowledge distillation. Facing above limitations, an intuitive question might be raised: *can we efficiently reuse the multi-grained knowledge in diverse features without retraining a heavy backbone for CISS?*

In this paper, we for the first time investigate the efficient multi-grained knowledge reuse for CISS by fusing multi-level features without retraining the heavy backbone. The rationale is that the fusion enables a better utilization of the prior knowledge to serve incremental learning tasks, i.e., better old knowledge preservation and new knowledge exploration as shown in Figure 2. Specifically, we first propose a simple multi-level feature aggregation module called naïve feature pyramid and apply it to a state-of-the-art method – MicroSeg [23]. The experimental results in Table I show that the fusion of high- and low-level features from any layer can boost the performance while aggregating all layers yields a new SOTA performance. This is reasonable as the low-level features (i) contain the well-learned prior knowledge; and (ii) offer more evident and detailed cues for objects/regions [3] with larger spatial dimensions, thereby producing better performance via feature fusion.

Furthermore, we advance the naïve feature pyramid by

TABLE I  
THE EFFECT OF LEVERAGING MULTI-LEVEL FEATURES ON THE SOTA CISS METHOD – MICROSEG-M [23]. ARCHITECTURE: DEEPLABV3 [4] WITH THE BACKBONE RESNET-101 [31].  $f_i, i \in \{1, 4\}$  IS THE FEATURE EXTRACTED FROM THE  $i^{th}$  BLOCK OF RESNET-101. SETTING: **15-5 (2 steps)** ON PASCAL VOC 2012. THE RESULTS INDICATE THAT FULLY EXPLORING THE MULTI-GRAINED KNOWLEDGE BY FUSING THE MULTI-LEVEL FEATURES IS VITAL FOR ENHANCING THE PERFORMANCE OF CISS.

Method	$f_1$	$f_2$	$f_3$	$f_4$	15-5 (2 steps)		
					0-15	16-20	all
MicroSeg-M [23]				✓	82.0	59.2	76.6
	✓			✓	82.6	60.3	77.3
		✓		✓	82.3	61.9	77.5
			✓	✓	82.1	59.3	76.7
	✓	✓		✓	82.5	59.3	77.0
	✓		✓	✓	82.3	58.9	76.7
	✓	✓	✓	✓	81.8	61.9	77.0
	✓	✓	✓	<b>82.7</b>	<b>62.8</b>	<b>78.0</b>	

proposing a novel **DE**nensely-interactive Feature **p**Yramid (**DEFY**) module (see Figure 3) for a better multi-level feature fusion. In particular, DEFY improves the fusion of high- and low-level features by allowing their dense interaction. Concretely, it establishes a per-pixel relationship between pairs of feature maps and then aggregates multi-pair outputs into an updated feature map. The per-pixel relationship between feature maps is established using an attention mechanism, where each pixel’s feature is weighted based on its similarity to the features of the neighboring pixels. This densely-interactive fusion enhances the complementary information provided by multi-level features, leading to more accurate semantic segmentation results.

We summarize our contributions as follows:

- To our knowledge, this is the first study to investigate reusing multi-grained knowledge efficiently by leveraging multi-level features without the need to retrain a heavy backbone for CISS. We empirically demonstrate that the utilization of multi-grained knowledge is essential for CISS and a simple aggregation of multi-level features using the naïve feature pyramid can significantly improve the baseline’s performance (**1.4%** mIoU gain).
- We further propose a novel densely-interactive feature pyramid (DEFY) module that enhances the fusion of multi-level features by enabling the establishment of per-pixel relationships and allowing for their dense interaction. We also discuss the differences between DEFY and other hierarchical feature aggregation approaches in Sec II-D.
- We show that the proposed DEFY can be easily integrated into three representative CISS models as a plug-in to enhance their performance. The scalability and ease of integration of DEFY make it a promising tool for advancing other fields of semantic segmentation.
- We conduct extensive experiments to evaluate the performance of the proposed DEFY, and the results demonstrate that it achieves a new state-of-the-art performance when integrated with the current SOTA CISS method.

## II. RELATED WORK

### A. Semantic Segmentation

Semantic segmentation [1]–[11], [32], [33] is a form of pixel-level prediction task that clusters parts of an image together which belong to the same object class. The introduction of Fully Convolutional Networks (FCN) [1] in 2015 marked a significant breakthrough in the field of semantic segmentation, and since then, numerous follow-up works have been proposed to improve the performance by introducing novel architectures, *e.g.*, Dilated Convolutions [34], Pyramid Pooling Module [2], U-Net [35], Atrous Spatial Pyramid Pooling (ASPP) [4], [5], and HRNet [33]. Generally, those methods all do per-pixel classification with a regular multi-class cross-entropy loss. In contrast, recent works [29], [36] reformulated semantic segmentation as a mask classification task, *i.e.*, predicting a set of binary masks, each of which is associated with a global class label. Despite the high performance in a close-set fashion, all mentioned methods suffer from *catastrophic forgetting* [12]–[14] when learning on new classes sequentially. This problem has raised the interest of researchers to develop semantic segmentation models that can learn incrementally. In this paper, we also follow this line to solve the incremental semantic segmentation task.

### B. Class Incremental Learning

Class incremental learning (CIL) aims to learn a classification model with the number of classes increasing sequentially. Existing methods can be mainly grouped into three categories: parameter isolation [17], [18], [37], [38], replay-based [39]–[44] and regularization-based methods [15], [41], [45]–[60]. Specifically, parameter isolation based approaches often assign independent parameters for each incremental task, but face an increasing amount of parameters with the number of tasks. Replay-based methods tend to either build a memory bank that stores a few samples of old classes [39]–[42] or learn a network to generate samples from old classes [43]. Those samples are further used to jointly train with new classes for preventing old knowledge forgetting. In contrast, regularization-based methods mainly focus on transferring old knowledge learned on old classes to the new model by knowledge distillation [16] or designing novel loss functions to prevent historical knowledge forgetting [56]–[59]. Note that the mentioned techniques are not mutually exclusive but complementary. In this paper, we propose an incremental learning method for semantic segmentation instead of classification.

### C. Class Incremental Semantic Segmentation

Class incremental semantic segmentation (CISS) is a similar task to CIL but aims to learn a segmentation model incrementally. Due to the similarity, the techniques in CIL can be leveraged by CISS, *e.g.*, knowledge distillation is used in ILT [24], MiB [25], SDR [61], PLOP [26], RCN [30], and DKD [47]; replay-based techniques are adopted by RECALL [62], SSUL-M [27], MicroSeg-M [23], and ALIFE [44]. However, CISS has its specific problem – background shift [25], *i.e.*, the background in the  $t^{th}$  step may contain old or future classes,

which cannot be solved by CIL methods. To that end, recent works have proposed two useful techniques: old knowledge based pseudo labeling [23], [26], [27] and unknown class modeling [23], [27]. This particular pseudo labeling complements the ground truth labels in the  $t^{th}$  step with pseudo labels of old classes predicted by the model of  $(t - 1)^{th}$  step while unknown class modeling tends to utilize a pre-trained class-agnostic model for possible objects detection and future class modeling. Despite the effectiveness, those methods exist some limitations: (i) the old knowledge in low-level features with much subtler details are overlooked when performing pseudo labeling and unknown class modeling [23], [27]; (ii) a heavy backbone is required to retrain in the incremental step [26], [30] when using multi-level features for knowledge distillation. In this paper, we propose to efficiently leverage the multi-grained knowledge in various features without retraining the parameters of backbone.

### D. Hierarchical Feature Aggregation

Hierarchical feature aggregation (HFA) [3], [63]–[82] is a widely used technique that involves leveraging the information present at different levels or scales within a deep model to learn more expressive representations, which can then be applied to various downstream tasks. Here, we mainly review different types of HFA in semantic segmentation [3], [63]–[78] and differentiate our method from the previous approaches. From the technical perspective, existing HFA approaches can be roughly divided into two categories, *i.e.*, multi-level feature aggregation (MFA) [3], [63], [65]–[69], [72], [73] and contextual feature aggregation (CFA) [74]–[78]. Specifically, MFA based approaches typically employ a feature pyramid construction strategy, where feature maps at different scales are utilized. These maps are processed through pyramidal pooling [3], [4] or dilated/atrous convolutions [5] to facilitate the aggregation process. The aggregation is often achieved by either gradually summing the multi-level feature maps [79], [83] or concatenating multi-level feature maps along the channel dimension [2], [4]. Our naïve feature pyramid used to examine the significance of leveraging multi-grained knowledge for CISS also follows this line of approach. In contrast, CFA based approaches offer a solution to model patch-wise relationships in a given image through using attention mechanisms, *e.g.*, Transformer-based architectures [74]–[78], [84], [85].

However, MFA based approaches overlook the interaction between pair-wise features by simply summing or concatenating multi-level features while CFA based approaches initially treat each patch in an image with equal attention without stressing the significant regions. In this paper, we focus on aggregating multi-level features for CISS and design a simple-yet-effective module that (i) explicitly builds the pair-wise and pixel-wise interaction between high- and low-level features; (ii) maintains the dominance of high-level knowledge while complementing it with diverse low-level knowledge by using high-level feature as the **Query** and low-level features as the **Key** and **Value** in an attention module; (iii) is a light-weight plug-and-play module that shows the effectiveness on three representative CISS methods.

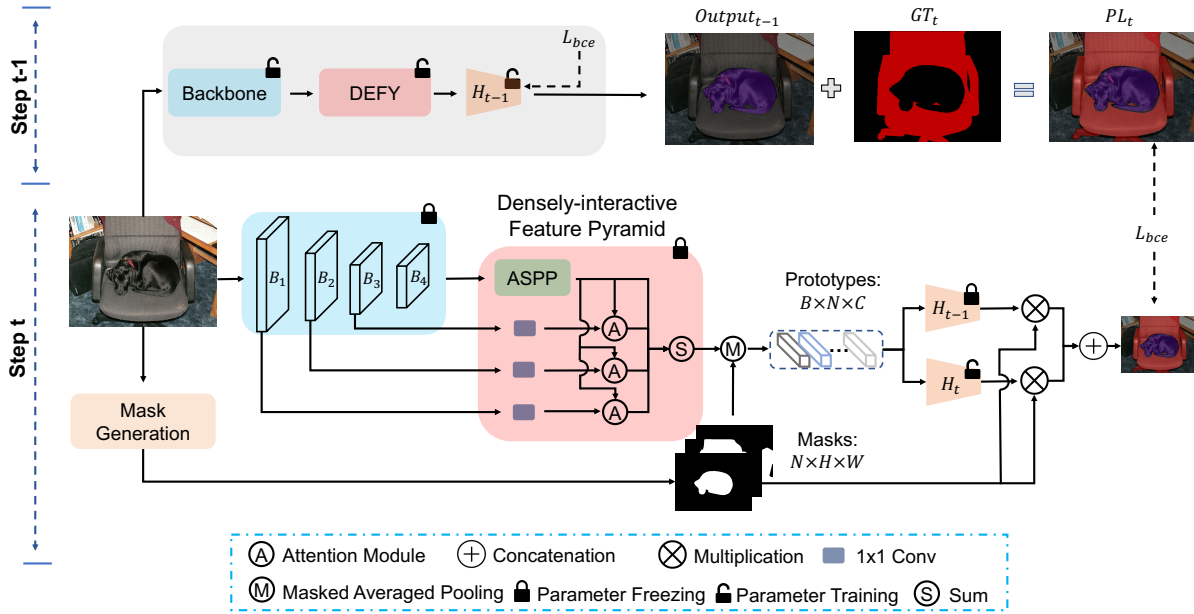


Fig. 3. The overview of applying our densely-interactive feature pyramid (DEFY) to the Mask2Former [29] based baseline method [23]. In the 1<sup>st</sup> step, the entire model including backbone, DEFY, and segmentation head  $H_1$  are trained on  $C_0$  classes. During training, DEFY builds pair-wise and pixel-wise interactions between high- and low-level features to capture and aggregate multi-grained knowledge. In the follow-up steps, only a new segmentation head  $H_t$  is trainable for  $C_t$  classes.  $C_t$ : the classes shown in step  $t$ .

### III. METHODOLOGY

#### A. Problem Set-up

Class incremental semantic segmentation (CISS) [23], [27] aims to learn a segmentation model incrementally by updating part/all of the parameters of the historical model and a set of new parameters specialized to the current task. Specifically, one CISS task often consists of  $T$  learning steps, each with a dataset  $D_t$  from  $C_t$  classes. Note that  $D_t$  may also contain historical classes from previous steps or future classes, but these classes are labeled as background, which results in a unique problem in CISS – *background shift*. Except background class, the given classes in the  $t^{\text{th}}$  step are disjoint with the classes from other steps, i.e.,  $C_t \cap C_i = \emptyset$ , where  $i \in \{1, \dots, T\} \setminus \{t\}$ . In step  $t$ , a model is learned on  $C_t$  classes only, the learned model tends to forget the historical knowledge acquired from old classes without accessing  $C_0 \cup \dots \cup C_{t-1}$  classes, thus causing *catastrophic forgetting* – the key problem in incremental learning. Overall, an incremental segmentation model is designed to tackle both *background shift* and *catastrophic forgetting*, thereby achieving good pixel-wise recognition performance on the current classes as well as the classes from the past steps, i.e.,  $C_0 \cup \dots \cup C_t$ .

#### B. Overview

In general, a CISS model consists of a heavy backbone  $F_b$  and  $T$  light-weight segmentation heads  $\{H_1, \dots, H_T\}$ , in which the  $F_b$  and  $H_1$  are fully trained in the 1<sup>st</sup> step and then  $[F_b \text{ and } H_t]$  or  $[only \ H_t]$  will be updated in step  $t$ . When learning the model in step  $t$ , it is common to borrow the old knowledge learned in step  $t-1$  by using the features of that model, e.g., four-level features extracted from four blocks of

ResNet-101 [31] – the standard backbone used in existing methods. The weakness of current CISS methods is that they either mine the prior knowledge stored in the high-level features only [23], [27]; or explore more knowledge in multi-level features but retrain the heavy backbone  $F_b$  [26], [30]. To that end, this work focuses on a better utilization of prior knowledge by efficiently leveraging multi-level features for improved CISS via training  $H_t$  only. Specifically, we propose to introduce a feature aggregation module between  $F_b$  and  $\{H_1, \dots, H_T\}$ . After a one-time training in the 1<sup>st</sup> step, the module can effectively fuse multi-level features for subsequent incremental segmentation tasks. For the module design, we first propose a naïve feature pyramid (NFP) module and apply it to the current SOTA method MicroSeg [23] to show a fusion of multi-level features can significantly boost its performance (refer to Table I). To advance the NFP, we further propose a novel densely-interactive feature pyramid (DEFY) module that does better feature aggregation by facilitating per-pixel relationship establishment and pair-wise interaction between features. Next, we will introduce each module in detail.

#### C. Naïve Feature Pyramid Module

Given the backbone – ResNet-101, we first extract four-level features  $\{f_1, f_2, f_3, f_4\}$  from four blocks. Following the previous CISS methods [23], we forward  $f_4$  to the ASPP [4], [5] module  $\phi$  to obtain the updated feature  $\phi(f_4)$ . This feature is derived from the multi-level aggregation by one Conv layer, three pooling pyramids and one ASPP pooling layer, which already has good abstract and global representations. However, leveraging  $f_4$  only may lack fine-grained details and local information that are necessary for accurately segmenting objects. For this reason, we aggregate low-level features to

$\phi(f_4)$  as a complementing. Concretely,  $f_1, f_2, f_3$  are projected into three 1x1 Conv layers  $\theta_1, \theta_2, \theta_3$ , separately, for the channel dimension reduction. Then, we concatenate all processed features as the new fused feature that serves as the input to the subsequent segmentation head. Since the processed features may have different spatial dimensions, we perform an up-sampling operation on some of them to ensure that they have the same spatial resolution as the others before concatenation. Overall, the process can be formulated as follows.

$$f^* = \text{Concat}\{\theta_1(f_1), \theta_2(f_2), \theta_3(f_3), \phi(f_4)\} \quad (1)$$

where  $f^*$  is the new fused feature,  $\theta_i$  the 1x1 Conv projection layer,  $\phi$  the ASPP module. Note that we omit the up-sampling operation for clarity. The detailed dimensions of features and Conv layers are given in Sec. IV-B.

1) *Preserving the Domination of High-level Features*: In principle, both high- and low-level features heritage the old knowledge from the model trained in the 1<sup>st</sup> step. Specifically, high-level features, e.g.,  $f_4$  in ResNet-101, contain abstract and global representations of an image that capture semantic information, which are important for accurately recognizing object categories. However, they may not capture fine-grained details and local information that are necessary for accurate object segmentation, which is why incorporating low-level features can be beneficial. To balance the dominance of high-level features and incorporating the fine-grained information of low-level features, we reduce the dimension of low-level features and then merge them with high-level ones, which is also used in DeepLabV3+ [3]. Moreover, this is more computationally efficient.

2) *The Difference from DeepLabV3+ [3]*: DeepLabV3+ [3] employs low- and high-level feature aggregation for semantic segmentation. This aggregation considers the feature of the first block and the output of ASPP only. Despite the similarity of structure, we propose the naïve feature pyramid particularly for CISS that highlights the multi-grained knowledge reuse for incremental tasks. In addition, we conduct extensive experiments to analyze each combination and show combining multi-level features achieves the best performance.

#### D. Densely-interactive Feature Pyramid Module

Building on the success of the naïve feature pyramid module for CISS, we propose an advanced densely-interactive feature pyramid (DEFY) module (Figure 3) that leverages attention mechanisms to achieve more effective feature fusion. Our DEFY considers both pair-wise and pixel-wise interactions between each pair of high- and low-level features, allowing it to preserve the dominance of high-level knowledge while simultaneously enriching the abstract high-level information with detailed low-level features. By considering these interactions, our method generates more comprehensive representations, which are particularly advantageous for incremental learning tasks. Concretely, we first project the feature dimension of low-level features  $\{f_1, f_2, f_3\}$  to the same dimension as the output of ASPP  $\phi(f_4)$  through three 1x1 Conv layers. Then, we enable the interaction of each pair of the low-level feature and  $\phi(f_4)$  via the attention block, in which  $\phi(f_4)$  is the **Query**

while the other serves as **Key** and **Value**. The formulation is defined as follows.

$$f_h^i = [\text{softmax}(\frac{(\phi(f_4)\omega_q)(\psi_i(f_i)\omega_k)^T}{\sqrt{d_k}})(\psi_i(f_i)\omega_v)]\omega_o \quad (2)$$

where  $\psi_i$  is the 1x1 Conv layer,  $i \in \{1, 2, 3\}$ ,  $\omega_{q,k,v}$  is the in-projection layer,  $\omega_o$  is the out-projection layer, and  $d_k$  is the in-projected dimension. Note that  $f_i \in \mathbb{R}^{b \times c \times h \times w}$  is reshaped to  $\mathbb{R}^{b \times h \times w \times c}$  as the input of the attention block, which is omitted for simplicity.

Regarding Eq.2, with  $\{f_1, f_2, f_3\}$ , we can obtain  $\{f_h^1, f_h^2, f_h^3\}$ . These features are then aggregated by summation as a new fused feature, which is shown below.

$$f^* = \text{Sum}\{f_h^1, f_h^2, f_h^3, \phi(f_4)\} \quad (3)$$

1) *Why DEFY is better?*: The strength of DEFY lies in its utilization of attention mechanisms, enabling the capture of crucial features for segmentation. More specifically, DEFY establishes per-pixel relationships between high- and low-level feature maps, and employs attention to assign weights to the contributions of different feature maps in the fused feature representation. This precise and effective combination of multi-level features results in enhanced segmentation performance, as the most relevant information is appropriately emphasized and utilized.

2) *Potential Variants of DEFY*: We acknowledge that DEFY can be reformulated in various ways. Here, we further investigate two extra variants, i.e., DEFY based on concatenation DEFY<sub>con</sub> and dual densely-interactive feature pyramid (D-DEFY) module. Specifically, DEFY<sub>con</sub> replaces the final summation operation with concatenation, which is similar to the naïve feature pyramid. In contrast, D-DEFY employs dual densely-interactive modules for each low- and high-level feature pair, where one module uses high-level feature as **Query** and low-level feature as **Key** and **Value**, and the other module uses the low-level feature as **Query** and high-level feature as **Key** and **Value**. Two outputs from dual densely-interactive modules are then fused by summation. Finally, we will combine the high-level feature  $\phi(f_4)$  with three fused outputs (from three pairs of features) via a summation operation as a new aggregated feature. We experiment with these variants and analyze the results in Sec. IV-G0d.

## IV. EXPERIMENTS

### A. Datasets

a) *PASCAL VOC 2012 [86]*: It is a widely used segmentation dataset, which can be repurposed for CISS. It contains 10,582/1,449 training/validation images from 21 classes including 20 object classes and one background class. We follow the previous works [23], [27], [30] to conduct experiments on multiple incremental tasks as shown in Table II. For example, in the **10-1 (11-steps)** task, a model is trained on 11 classes (including the background class) in the 1<sup>st</sup> step, and then sequentially trained on one new class from step 2 to step 11. Note that all experiments are under the more realistic *overlapped* set-up as per [23], [26], [27], [30], i.e., the background of an image in step  $t$  may contain old or future

classes while only the new classes belonging to the  $t^{\text{th}}$  step are labeled, except for Sec. IV-G0e that evaluates our method in the *disjoint* set-up, which assumes all future classes are known and *not* shown in the background.

b) *ADE20K* [87]: This is a more challenging semantic segmentation dataset with 150 classes for daily life scenes, which contains 20,210/2,000 training/validation images. The experimental protocol for ADE20K is in line with that of PASCAL VOC 2012.

## B. Implementation Details

a) *Training and Inference*: To verify the effectiveness of the proposed DEFY, we apply it to three representative methods, *i.e.*, MiB (CVPR2020) [25], SSUL (NeurIPS2021) [27] and MicroSeg (NeurIPS2022) [23]. Their official codes are open-source. For a fair comparison, we follow their implementations for training and inference and apply our light-weight plug-in DEFY to them. We also offer their implementation details below.

All three methods adopt DeepLabV3 [4] with a ResNet-101 backbone, which is pre-trained on ImageNet [88].

**For MiB [25]**: Following [5], they use the SGD optimizer with the same momentum and weight decay. The initial learning rate for the 1<sup>st</sup> step is 1e-2 and 1e-3 for the follow-up steps, scheduled by “poly” learning rate policy [4]. The model is trained with a batch size 24 for 30 epochs on PASCAL VOC 2012, and for 60 epochs on ADE20K during each learning step. The data augmentations used here are random scaling (from 0.5 to 2.0) and random flipping.

**For SSUL [27]**: The optimizer, learning rate schedule, data augmentation and the initial learning rate for the first step are same as [25], but the initial learning rate for the following steps is 1e-2 for SSUL. The batch size 32 and epochs 50 are used on PASCAL VOC 2012 while batch size 24 and epochs 60 on ADE20K. The detector of saliency map leveraged in SSUL is DSS [28] pre-trained on MSRA-B dataset [89].

**For MicroSeg [23]**: Except for the same optimizer, learning rate schedule and data augmentation as that in [23], [25], MicroSeg uses the initial learning rate 1e-2 and batch size 16 for PASCAL VOC 2012 while 5e-3 and 12 for ADE20K in all steps. The proposal generator is Mask2Former [29] pre-trained on MS-COCO [90], which produces 100 class-agnostic proposals for each image. It’s worth noting that the proposal generator is not fine-tuned on any benchmark dataset for a fair comparison. The hyper-parameters for Micro mechanism are  $K = 5$  for PASCAL VOC 2012 and  $K = 1$  for ADE20K. When using replaying, the samples of extra memory is 100 for PASCAL VOC 2012.

b) *Architecture Details*: Following existing works [23], [25]–[27], [30], we use DeepLabV3 [4] with ResNet-101 backbone. Given the input image size  $513 \times 513$ , the dimensions of four-level features from ResNet-101 are listed below.

$$\begin{aligned} f_1 &\in \mathbb{R}^{b \times 256 \times 128 \times 128}, f_2 \in \mathbb{R}^{b \times 512 \times 64 \times 64}, \\ f_3 &\in \mathbb{R}^{b \times 1024 \times 32 \times 32}, f_4 \in \mathbb{R}^{b \times 2048 \times 32 \times 32}. \end{aligned}$$

The output of ASPP is  $\phi(f_4) \in \mathbb{R}^{b \times 256 \times 32 \times 32}$ .

In naïve feature pyramid, the channel dimension of the three 1x1 Conv layers are  $\theta_1 \in \mathbb{R}^{256 \times 48}$ ,  $\theta_2 \in \mathbb{R}^{512 \times 48}$ ,  $\theta_3 \in \mathbb{R}^{1024 \times 48}$ , respectively. The up-sampling operation will enlarge the spatial dimension of other features to the same dimension of  $f_1$ , *i.e.*,  $128 \times 128$ . After concatenation, the dimension of the final output is  $\mathbb{R}^{b \times 400 \times 128 \times 128}$ .

For our DEFY, the channel dimensions of the three 1x1 Conv layers are  $\psi_1 \in \mathbb{R}^{256 \times 256}$ ,  $\psi_2 \in \mathbb{R}^{512 \times 256}$ ,  $\psi_3 \in \mathbb{R}^{1024 \times 256}$ , respectively. Three in-projection layers  $\omega_{q,k,v}$  share the same dimension  $\mathbb{R}^{256 \times 768}$  while the out-projection layer recovers the original input dimension with a linear projection ( $\mathbb{R}^{768 \times 256}$ ).

## C. Compared Methods

We compare all existing methods for a comprehensive evaluation. Specifically, three classical methods in CIL, *i.e.*, EWC [52], Lwf-MC (TPAMI2017) [15], and ILT (ICCVW2019) [24], are repurposed for CISS and compared. Moreover, we make comparison with the existing state-of-the-art CISS methods including MiB (CVPR2020) [25], SDR (CVPR2021) [61], PLOP (CVPR2021) [26], RCIL (CVPR2022) [30], SSUL (NeurIPS2021) [27], DKD (NeurIPS2022) [47], ALIFE (NeurIPS2022) [44], MicroSeg (NeurIPS2022) [23], and EWF (CVPR2023) [91].

## D. Evaluation Metric

We evaluate our method using the mean Intersection-over-Union (mIoU) metric, which is computed as the average of the Intersection-over-Union (IoU) scores for each class. The IoU score for a class is computed as the true positives divided by the sum of true positives, false positives, and false negatives. In all tables, we reports three mIoU metrics: the mIoU of the classes in the first step, the mIoU of the classes in the follow-up steps and the mIoU of all classes. The first metric evaluates the model’s ability to preserve old knowledge, while the second measures its ability to learn new classes. The final metric reflects the model’s overall performance on both old and new classes.

## E. Results on PASCAL VOC 2012

Table II shows the results on PASCAL VOC 2012. Overall, our DEFY can always boost the performance of the baseline methods significantly except for two cases with comparable performance, and a new state-of-the-art performance is achieved when combined with the current SOTA MicroSeg. In addition, we also make several interesting observations. First, the proposed DEFY is particularly effective in improving the performance of baseline methods that have poor original performance. For example, it improves MiB by 44.1% on **10-1 (11 steps)**, 37.9% on **15-1 (6 steps)**, 3.8% on **5-3 (6 steps)** and 5.1% on **19-1 (2 steps)**. This is because MiB does not employ pseudo labeling or modeling of unknown classes, thereby fully leveraging the multi-grained old knowledge to enhance the power of feature representation is especially vital for it. Second, adding our DEFY to the baselines wins in the most cases on both mIoU (1<sup>st</sup> step) and mIoU in the following steps,

TABLE II

COMPARISON ON PASCAL VOC 2012. THE PROPOSED AFP IMPROVES THREE REPRESENTATIVE METHODS SIGNIFICANTLY IN MOST CASES. THE BEST PERFORMANCE IS IN **bold**.

Method	10-1 (11 steps)			2-2 (10 steps)			15-1 (6 steps)			5-3 (6 steps)			19-1 (2 steps)			15-5 (2 steps)		
	0-10	11-20	all	0-2	2-18	all	0-15	16-20	all	0-5	6-20	all	0-19	20	all	0-15	16-20	all
EWC [52] (NAC17)	-	-	-	-	-	-	0.3	4.3	1.3	-	-	-	26.9	14.0	26.3	24.3	35.5	27.1
LwF-MC [15] (TPAMI17)	4.7	5.9	4.9	3.5	4.7	4.5	6.4	8.4	6.9	20.9	36.7	24.7	64.4	13.3	61.9	58.1	35.0	52.3
ILT [24] (ICCVW19)	7.2	3.7	5.5	5.8	5.0	5.1	8.8	8.0	8.6	22.5	31.7	29.0	67.8	10.9	65.1	67.1	39.2	60.5
SDR [61] (CVPR21)	32.1	17.0	24.9	13.0	5.1	6.2	44.7	21.8	39.2	12.1	6.5	8.1	69.1	32.6	67.4	57.4	52.6	69.9
PLOP [26] (CVPR21)	44.0	15.5	30.5	24.1	11.9	13.7	65.1	21.1	54.6	17.5	19.2	18.7	75.4	37.4	73.5	75.7	51.7	70.1
RCIL [30] (CVPR22)	55.4	15.1	34.3	-	-	-	70.6	23.7	59.4	-	-	-	-	-	-	78.8	52.0	72.4
ALIFE [44] (NeurIPS22)	-	-	-	-	-	-	64.4	34.9	57.4	-	-	-	76.6	<b>49.4</b>	75.3	77.2	52.5	71.3
DKD [47] (NeurIPS22)	-	-	-	-	-	-	78.1	<b>42.7</b>	69.7	-	-	-	77.8	41.5	76.0	78.8	<b>58.2</b>	73.9
EWf [91] (CVPR23)	71.5	30.3	51.9	-	-	-	77.7	32.7	67.0	61.7	42.2	47.7	77.9	6.7	74.5	-	-	-
MiB [25] (CVPR20)	12.3	13.1	12.7	41.1	23.4	25.9	34.2	13.5	29.3	57.1	42.6	46.7	71.4	23.6	69.2	76.4	50.0	70.1
+ Ours	70.7	41.5	56.8	55.9	23.2	27.9	76.3	38.2	67.2	68.5	43.3	50.5	76.7	25.2	74.3	77.0	49.0	70.4
SSUL [27] (NeurIPS21)	71.3	46.0	59.3	62.4	42.5	45.3	77.3	36.6	67.6	72.4	50.7	56.9	77.7	29.7	75.4	77.8	50.1	71.2
+ Ours	73.4	47.8	61.2	61.9	42.1	45.0	77.6	37.3	68.0	72.2	51.4	57.3	77.9	27.4	75.5	78.1	51.9	71.9
MicroSeg [23] (NeurIPS22)	72.6	48.7	61.2	61.4	40.6	43.5	<b>80.1</b>	36.8	<b>69.8</b>	77.6	59.0	64.3	78.8	14.0	75.7	80.4	52.8	73.8
+ Ours	<b>73.9</b>	<b>48.9</b>	<b>62.0</b>	<b>69.3</b>	<b>52.0</b>	<b>54.5</b>	79.8	31.4	68.3	<b>79.8</b>	<b>60.4</b>	<b>65.9</b>	<b>81.4</b>	11.1	<b>78.1</b>	<b>81.5</b>	53.0	<b>74.7</b>
Joint (Upper bound)	82.1	79.6	80.9	76.5	81.6	80.9	82.7	75.0	80.9	81.4	80.7	80.9	81.0	79.1	80.9	82.7	75.0	80.9

TABLE III

COMPARISON ON ADE20K. THE PROPOSED AFP IMPROVES THE BASELINE METHODS SIGNIFICANTLY IN MOST CASES. THE BEST PERFORMANCE IS IN **bold**.

Method	100-5 (11 steps)			100-10 (6 steps)			100-50 (2 steps)		
	0-100	101-150	all	0-100	101-150	all	0-100	101-150	all
ILT [24] (ICCVW19)	0.1	1.3	0.5	0.1	3.1	1.1	18.3	14.4	17.0
PLOP [26] (CVPR21)	39.1	7.8	28.8	40.5	13.6	31.6	41.9	14.9	32.9
ALIFE [44] (NeurIPS22)	-	-	-	41.0	<b>22.8</b>	35.0	42.2	<b>23.1</b>	35.9
DKD [47] (NeurIPS22)	-	-	-	41.6	19.5	34.3	42.4	22.9	36.0
EWf [91] (CVPR23)	41.4	13.4	32.1	41.5	16.3	33.2	41.2	21.3	34.6
MiB [25] (CVPR20)	36.0	5.7	26.0	38.2	11.1	29.2	40.5	17.2	32.8
+ Ours	38.6	14.9	30.8	39.3	17.4	32.0	40.0	16.7	32.3
SSUL [27] (NeurIPS21)	39.9	17.4	32.5	40.2	18.8	33.1	41.3	18.0	33.6
+ Ours	39.8	19.0	32.9	40.0	19.9	33.4	41.0	20.3	34.1
MicroSeg [23] (NeurIPS22)	40.4	20.5	33.8	41.5	21.6	34.9	40.2	18.8	33.1
+ Ours	<b>43.0</b>	<b>20.9</b>	<b>38.6</b>	<b>43.1</b>	22.7	<b>36.3</b>	<b>43.3</b>	21.7	<b>36.2</b>
Joint (Upper bound)	43.8	28.9	38.9	43.8	28.9	38.9	43.8	28.9	38.9

*i.e.*, 83.3% (15/18) and 66.7% (12/18), respectively, which indicates our DEFY improves both old knowledge preservation and new knowledge exploration.

Moreover, Figure 4 shows the qualitative comparison, which is consistent with the quantitative results. In general, our DEFY can significantly improve the quality of the baselines, except for MicroSeg where it mis-classifies a “sofa” with a similar shape to a train as a “train”.

#### F. Results on ADE20K

Table III shows the results on a more challenging dataset – ADE20K with more diverse classes (150 classes). Overall, our DEFY can improve the baseline methods with remarkable performance gains in most cases. In particular, we found that our DEFY can improve MicroSeg the most when trained on 100 classes in the 1<sup>st</sup> step, *e.g.*, 4.8% on **100-5 (11 steps)**, 3.1% on **100-50 (2 steps)**, and 1.4% on **100-10 (6 steps)**. The reason is that the better pseudo labeling and unknown class modeling in MicroSeg requires a more powerful representation of feature, which is achieved by the dense interaction based multi-level feature fusion in our DEFY. Moreover, we can see

that our DEFY can enhance the old knowledge preservation in 5 out of 9 cases and improve the new knowledge exploration in 8 out of 9 cases. This manifests that our DEFY can benefit more on novel class recognition where larger number of classes exist.

#### G. Further Analysis

*a) The Effect of Replaying:* Following MicroSeg [23], we also verify the effectiveness of the proposed method when an extra memory bank (fixed size=100 [23], [27]) for replaying is used, as shown in Table IV. We found that our DEFY can benefit more with replaying, *e.g.*, performance gains are **3.9%** vs. 2.8% on **15-5 (2 steps)** and **7.5%** vs. 4.6% on **15-1 (6 steps)** comparing to the baseline. This indicates that the old knowledge reuse via multi-level feature fusion can works better when using memory based replaying.

*b) Step-wise mIoU:* Figure 5 shows the step-wise mIoU under **15-1 (6 steps)**, from which we can see that with the DEFY the baseline consistently achieves higher performance in each step, except for the case of *MicroSeg+Ours*, where the performance is comparable in terms of mIoU. From the figure,

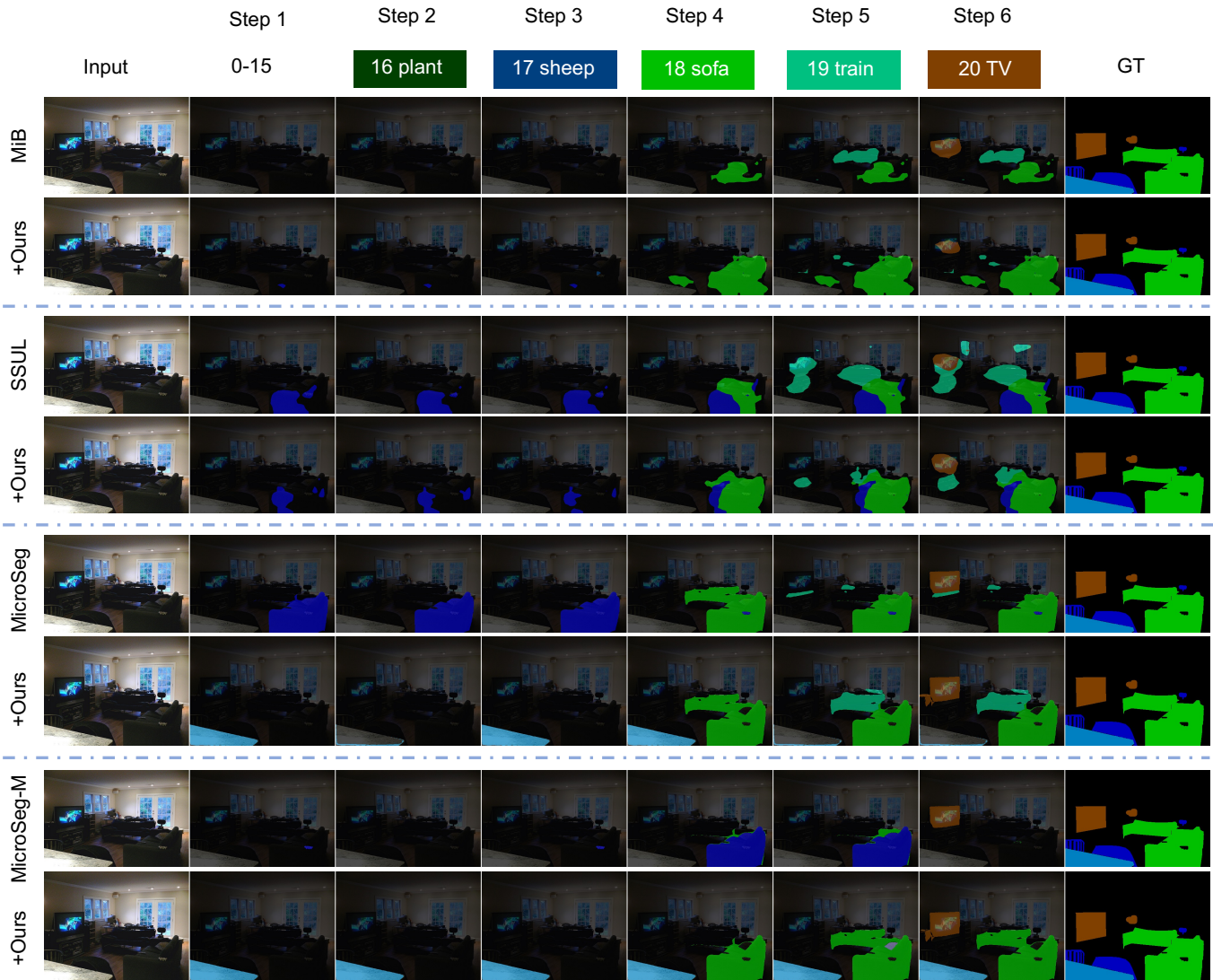


Fig. 4. Qualitative comparison with baseline methods on 15-1 (6 steps) setting on PASCAL VOC 2012. Zoom in for details.

TABLE IV  
THE EFFECT OF REPLAYING ON PASCAL VOC 2012.

Method	15-5 (2 steps)			15-1 (6 steps)		
	0-15	16-20	all	0-15	16-20	all
MicroSeg	80.4	52.8	73.8	80.1	36.8	69.8
+ Ours	81.5	53.0	74.7	79.8	31.4	68.3
MicroSeg-M	82.0	59.2	76.6	81.3	52.5	74.4
+ Ours	<b>82.8</b>	<b>65.2</b>	<b>78.6</b>	<b>81.8</b>	<b>56.5</b>	<b>75.8</b>

we found that *MicroSeg+Ours* performs better in the 4<sup>th</sup> step, but worse on step 5 (class “TV”). The possible reason is that *MicroSeg+Ours* is prone to segment “TV” wrongly compared with *MicroSeg*.

We further show the averaged mIoU and its standard deviation (STD) over 6 steps in Figure 6. Interestingly, we found that our DEFY enables higher performance and lower STD when applied to *MiB*, *SSUL* and *MicroSeg-M*. This manifests the DEFY can enhance those baselines in terms

of both performance and stability. Moreover, *MicroSeg+Ours* demonstrates a similar averaged mIoU and STD though it performs worse in the final step (see Figure 5).

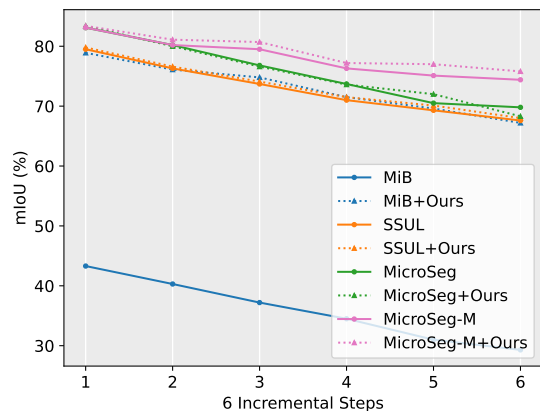


Fig. 5. Step-wise mIoU on PASCAL VOC 2012 under 15-1 (6 steps) set-up.

TABLE V  
THE CLASS-WISE IOU ON PASCAL VOC 2012 UNDER ALL THE INCREMENTAL SET-UPS. WE COMPARE WITH THE CURRENT SOTA METHOD – MICROSEG [23] AND ITS REPLAYING-BASED VERSION.

Method	bg	aero	bike	bird	boat	bottle	bus	car	cat	chair	cow	table	dog	horse	mbike	person	plant	sheep	sofa	train	TV	mIoU
<b>10-1 (11 steps)</b>																						
MicroSeg [23]	<b>89.7</b>	91.6	<b>41.2</b>	<b>95.1</b>	74.1	<b>84.4</b>	<b>90.3</b>	89.6	86.8	37.4	18.6	<b>33.4</b>	75.1	38.5	<b>76.6</b>	87.9	15.7	34.1	<b>28.5</b>	<b>60.0</b>	<b>37.0</b>	61.2
+Ours	83.1	<b>92.5</b>	40.9	87.9	<b>75.6</b>	78.7	76.2	<b>91.0</b>	<b>94.7</b>	<b>44.8</b>	<b>47.2</b>	28.7	<b>82.3</b>	<b>60.4</b>	75.5	<b>88.3</b>	<b>20.1</b>	<b>42.8</b>	27.7	42.1	21.5	<b>62.0</b>
MicroSeg-M [23]	<b>90.9</b>	86.8	42.0	91.5	<b>78.0</b>	<b>84.0</b>	90.9	87.6	89.3	40.1	<b>68.8</b>	47.5	69.4	40.4	84.9	85.7	<b>34.0</b>	45.2	<b>33.6</b>	70.8	61.6	67.8
+Ours	88.4	<b>92.0</b>	<b>43.3</b>	<b>92.0</b>	73.4	78.4	<b>94.1</b>	<b>89.9</b>	<b>95.7</b>	<b>46.0</b>	68.7	<b>48.1</b>	<b>81.1</b>	<b>65.0</b>	<b>85.5</b>	<b>86.4</b>	31.3	<b>52.7</b>	27.5	<b>77.1</b>	<b>61.7</b>	<b>70.4</b>
<b>2-2 (10 steps)</b>																						
MicroSeg [23]	85.7	73.9	24.4	40.8	25.9	48.8	<b>27.7</b>	74.9	48.0	4.7	39.3	5.1	54.8	<b>44.5</b>	67.1	80.5	11.8	38.0	27.0	<b>45.2</b>	<b>47.0</b>	43.5
+Ours	<b>86.0</b>	<b>89.2</b>	<b>32.8</b>	<b>71.8</b>	<b>45.9</b>	<b>65.5</b>	27.5	<b>80.8</b>	<b>77.0</b>	<b>17.4</b>	<b>49.2</b>	<b>47.0</b>	<b>63.2</b>	35.3	<b>74.6</b>	<b>82.3</b>	<b>34.2</b>	<b>59.5</b>	<b>27.0</b>	41.7	35.7	<b>54.5</b>
MicroSeg-M [23]	<b>87.2</b>	72.8	20.2	39.2	34.2	59.1	79.5	<b>82.1</b>	78.3	6.6	35.3	13.5	<b>69.4</b>	<b>47.9</b>	69.7	80.1	25.9	56.0	<b>28.1</b>	70.5	41.0	52.2
+Ours	87.0	<b>90.0</b>	<b>29.4</b>	<b>66.1</b>	<b>48.9</b>	<b>66.6</b>	<b>87.4</b>	81.6	<b>80.8</b>	<b>17.7</b>	<b>49.4</b>	41.4	64.5	46.6	<b>74.8</b>	<b>82.0</b>	<b>35.1</b>	<b>72.4</b>	25.1	<b>72.1</b>	<b>55.4</b>	<b>60.7</b>
<b>15-1 (6 steps)</b>																						
MicroSeg [23]	<b>89.8</b>	<b>92.9</b>	<b>44.4</b>	<b>95.5</b>	76.0	82.8	<b>92.9</b>	90.9	93.4	<b>48.6</b>	68.2	52.9	89.8	83.5	<b>89.7</b>	90.4	11.7	<b>56.2</b>	<b>24.8</b>	<b>57.3</b>	<b>34.2</b>	<b>69.8</b>
+Ours	82.4	<b>93.7</b>	43.4	91.2	<b>78.9</b>	<b>87.9</b>	<b>88.8</b>	<b>91.8</b>	<b>93.9</b>	39.5	<b>71.2</b>	<b>55.5</b>	<b>91.5</b>	<b>91.3</b>	89.0	<b>91.0</b>	<b>21.9</b>	53.8	22.5	43.9	14.9	<b>68.3</b>
MicroSeg-M [23]	<b>91.2</b>	93.2	43.4	<b>93.1</b>	<b>78.7</b>	84.7	<b>91.9</b>	<b>91.0</b>	94.3	<b>45.8</b>	<b>88.4</b>	56.0	88.5	84.6	86.9	90.1	22.9	71.5	<b>31.0</b>	71.5	<b>65.6</b>	74.4
+Ours	90.5	<b>93.5</b>	<b>43.5</b>	91.7	77.3	<b>85.4</b>	91.4	90.9	<b>95.6</b>	38.5	87.5	<b>59.6</b>	<b>90.8</b>	<b>91.6</b>	<b>90.4</b>	<b>90.9</b>	<b>45.9</b>	<b>75.5</b>	26.3	<b>75.8</b>	58.9	<b>75.8</b>
<b>5-3 (6 steps)</b>																						
MicroSeg [23]	<b>89.1</b>	91.2	34.8	<b>89.3</b>	73.9	<b>87.3</b>	<b>82.3</b>	<b>83.6</b>	79.6	4.6	<b>55.5</b>	40.0	76.6	55.5	74.1	<b>87.9</b>	31.2	51.4	<b>30.5</b>	<b>70.2</b>	<b>62.7</b>	64.3
+Ours	86.4	<b>93.7</b>	<b>43.1</b>	89.2	<b>79.4</b>	86.8	75.8	78.6	<b>86.5</b>	<b>14.3</b>	52.0	<b>49.3</b>	<b>79.6</b>	<b>60.9</b>	<b>83.8</b>	85.7	<b>45.6</b>	<b>63.3</b>	22.1	61.7	46.1	<b>65.9</b>
MicroSeg-M [23]	<b>90.9</b>	81.2	34.7	87.8	67.4	<b>87.0</b>	85.0	78.2	80.6	<b>21.8</b>	55.1	37.9	77.3	52.9	74.5	86.2	43.4	38.8	<b>33.8</b>	74.8	67.0	64.6
+Ours	89.5	<b>93.6</b>	<b>44.1</b>	<b>94.4</b>	<b>78.4</b>	86.8	<b>87.8</b>	<b>79.0</b>	<b>86.2</b>	16.7	<b>55.8</b>	<b>49.5</b>	<b>82.2</b>	<b>59.6</b>	<b>79.9</b>	<b>87.3</b>	<b>43.8</b>	<b>58.6</b>	32.5	<b>79.0</b>	<b>69.3</b>	<b>69.2</b>
<b>19-1 (2 steps)</b>																						
MicroSeg [23]	<b>88.8</b>	87.5	41.4	<b>92.5</b>	72.6	85.3	<b>96.0</b>	85.6	94.9	36.6	92.4	57.6	<b>90.9</b>	89.6	85.0	89.9	71.6	82.2	50.4	<b>87.0</b>	<b>13.9</b>	75.7
+Ours	<b>88.0</b>	<b>93.5</b>	<b>44.8</b>	<b>92.3</b>	<b>77.6</b>	<b>87.2</b>	<b>94.3</b>	<b>91.5</b>	<b>95.2</b>	<b>42.3</b>	<b>93.3</b>	<b>60.6</b>	<b>90.9</b>	<b>91.4</b>	<b>88.6</b>	<b>91.5</b>	<b>74.7</b>	<b>89.9</b>	<b>54.1</b>	<b>86.5</b>	11.1	<b>78.1</b>
MicroSeg-M [23]	93.6	86.8	43.7	87.5	73.3	84.0	<b>96.1</b>	90.5	93.8	37.3	87.8	<b>62.9</b>	<b>90.4</b>	88.6	88.6	89.9	71.0	83.0	51.5	85.9	<b>62.9</b>	78.5
+Ours	<b>93.9</b>	<b>93.8</b>	<b>44.1</b>	<b>92.1</b>	<b>77.5</b>	<b>86.6</b>	94.2	<b>91.5</b>	<b>95.1</b>	<b>44.7</b>	<b>92.8</b>	61.4	89.3	<b>91.6</b>	<b>88.7</b>	<b>91.5</b>	<b>74.1</b>	<b>90.3</b>	<b>52.7</b>	<b>86.6</b>	48.0	<b>80.0</b>
<b>15-5 (2 steps)</b>																						
MicroSeg [23]	<b>91.7</b>	91.1	<b>44.8</b>	92.4	<b>80.1</b>	<b>85.2</b>	93.3	<b>91.3</b>	94.5	<b>43.0</b>	69.3	55.9	<b>90.5</b>	83.9	90.1	90.1	<b>32.3</b>	62.3	<b>30.6</b>	82.0	<b>57.0</b>	73.8
+Ours	89.6	<b>91.9</b>	43.2	<b>93.0</b>	78.2	85.0	<b>94.2</b>	90.2	<b>96.3</b>	38.7	<b>82.8</b>	<b>60.1</b>	90.2	<b>90.6</b>	<b>90.2</b>	<b>90.3</b>	26.1	<b>72.6</b>	29.4	<b>82.4</b>	54.5	<b>74.7</b>
MicroSeg-M [23]	<b>93.0</b>	<b>91.5</b>	42.9	<b>94.0</b>	<b>80.1</b>	85.4	92.2	<b>91.8</b>	94.7	44.5	<b>89.5</b>	55.2	90.1	87.8	<b>90.3</b>	90.5	48.0	<b>76.5</b>	36.1	77.6	58.0	76.6
+Ours	92.9	<b>91.5</b>	<b>45.8</b>	91.4	77.6	<b>85.8</b>	<b>93.4</b>	90.7	<b>96.2</b>	<b>46.3</b>	88.5	<b>61.2</b>	<b>90.6</b>	<b>91.1</b>	90.1	<b>90.7</b>	<b>53.6</b>	83.4	<b>38.2</b>	<b>81.6</b>	<b>69.4</b>	<b>78.6</b>

c) *Class-wise IoU*: We show the class-wise IoU under all incremental set-ups on PASCAL VOC 2012 in Table V. Overall, our DEFY can benefit the baseline methods in most cases. The detailed analysis for each incremental set-up is given as follows.

**10-1 (11 steps)**: We found *MicroSeg + Ours* outperforms *MicroSeg* on 11 classes out of 21 classes, often by large margins. For example, in 21 classes, the improvement higher than 5% is 6. When using replaying, *MicroSeg-M + Ours* wins in 15 classes, which indicates that our DEFY can benefit more with a small extra memory bank.

**2-2 (10 steps)**: In this most challenging set-up where only 3 classes (with one background class) are used to train the entire model in the 1<sup>st</sup> step, our method shows the most significant improvements, e.g., 11.0% on *MicroSeg* and 8.5% on *MicroSeg-M*. In particular, *MicroSeg + Ours* surpasses the baseline in 17 out of 21 classes, often by large margins, while *MicroSeg - M + Ours* wins in 16 out of 21 classes. This demonstrates that the DEFY can effectively benefit a baseline method in more challenging incremental scenarios.

**15-1 (6 steps)**: Our DEFY does not benefit the baseline method when adding on *MicroSeg*, but with comparable performance. Specifically, in 10 out of 21 classes, *MicroSeg + Ours* outperforms *MicroSeg*. We found the weaker performance is mainly due to the poor segmentation results on class “TV” where *MicroSeg* surpasses our method by 19.3%. This can be mitigated by replaying, which narrows the gap to 6.7%. Moreover, with replaying, our method outperforms the baseline *MicroSeg-M*. This manifests that our method can make better use of an extra memory bank.

**5-3 (6 steps)**: This is the third most challenging set-up regarding the mIoU. Our DEFY enhances the performance of both the two baselines regardless of whether the replaying is

employed or not. Interestingly, we found the replaying brings limited improvement on *MicroSeg*, i.e., 0.3% mIoU gain. In contrast, with our DEFY, the improvement becomes larger, i.e., 3.3% mIoU gain. This is encouraging as our DEFY can boost the capability of the baseline method to use an extra memory bank for replaying.

**19-1 (2 steps)**: This is a relatively simpler set-up as most of the classes, i.e., 20 classes (including one background class), are used to train the model in step 1. We found *MicroSeg/MicroSeg-M* has already performed well in this set-up with the highest mIoU among all set-ups. Nevertheless, our DEFY can further boost the performance of the baseline methods with significant mIoU gains, i.e., 2.4% on *MicroSeg* and 1.5% on *MicroSeg-M*. It’s worth noting that the performance of *MicroSeg - M + Ours* approaches the oracle’s performance, with only 0.9% mIoU gap.

**15-5 (2 steps)**: In this set-up, except for the better overall performance compared with two baselines, our method wins 11 out of 21 classes on *MicroSeg* while 14/21 on *MicroSeg-M*. Moreover, our method can also better use of the extra memory bank with 3.9% mIoU gain against 2.8% (baseline).

d) *Variants of Feature Aggregation Module*: As mentioned in Sec. III-D2, the feature aggregation can be formed in various ways. We show the ablation study in Table VI for comparison of several variants. A few observations can be made here. (i) All of the variant modules have a light-weight architecture, with the parameters occupying less than 3.2% of the original training parameters. It’s worth noting that the variant modules only undergo one-time training in step 1, so this comparison is made based on step 1. (ii) Using concatenation to replace summation after the output of the attention module (as in DEFY<sub>con</sub>) can improve the baseline’s performance, but it performs worse than DEFY with summation. (iii) Dual densely-

interactive Feature Pyramid (D-DEFY) (refer to Sec. III-D2 for details) does not benefit DEFY more. The reason for the lower performance of D-DEFY compared to DEFY may be due to the addition of the output of one attention module with the low-level feature as the **Query** to the other with the high-level feature as the **Query**, which could damage the dominance of the high-level feature that contains the essential abstract and global representation needed for accurate segmentation.

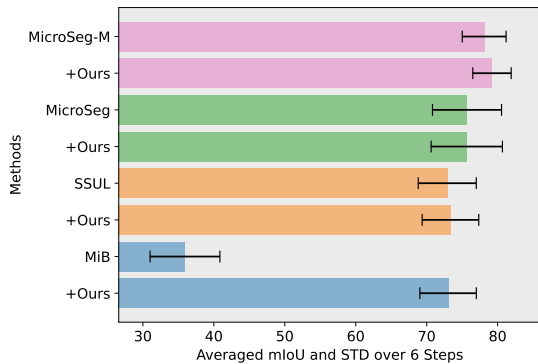


Fig. 6. Averaged mIoU over 6 steps (15-1 PASCAL VOC 2012).

TABLE VI

COMPARISON OF VARIOUS ARCHITECTURES FOR FEATURE AGGREGATION MODULE ON PASCAL VOC 2012. NFP: NAÏVE FEATURE PYRAMID. DEFY: DENSELY-INTERACTIVE FEATURE PYRAMID.

Variant	15-5 (2 steps)			#Param <sub>add</sub> / #Param <sub>ori</sub> (%)
	0-15	16-20	all	
MicroSeg-M	82.0	59.2	76.6	-
+ NFP	82.7	62.8	78.0	0.2% (0.1M/62.1M)
+ DEFY <sub>con</sub>	82.1	63.6	77.7	2.1% (1.3M/62.1M)
+ D-DEFY	82.3	61.6	77.4	3.1% (1.9M/62.1M)
+ DEFY	<b>82.8</b>	<b>65.2</b>	<b>78.6</b>	1.9% (1.2M/62.1M)

e) *Evaluation in the Disjoint Set-up*: Some past works [25], [26], [30] also evaluate their methods in the *disjoint* set-up, which is less realistic as it assumes that all future classes are known and *not* shown in the background of the current step. For a comprehensive comparison, we also verify the effectiveness of our method in this set-up (Table VII), from which we found the proposed DEFY can consistently improve the baselines, often by large margins.

f) *Failure Cases*: We present some failure cases in Figure 7 to investigate the limitations of our method and identify potential avenues for future research. We found that failures often occur in two scenarios. First, pixel-level annotations in ground-truth masks are ambiguous, e.g., the “chair” shares the similar appearance to the “sofa”, but labeled as the “chair” class (the 1<sup>st</sup> two rows). Consequently, when the model classifies a chair with a similar shape to a sofa as “sofa”, the IoU for that prediction is zero. This requires a correction of the dataset. Second, our method tends to miss the small objects, e.g., the “person” in the corner of an office (the 3<sup>rd</sup> row), the “person” (a small face photo) on a train (the 4<sup>th</sup> row), the “car” on a screen of a building (the last row). However, correctly classifying small objects is a common challenge for

TABLE VII  
THE EVALUATION IN THE *disjoint* SET-UP ON PASCAL VOC 2012.

Method	15-5 (2 steps)			15-1 (6 steps)		
	0-15	16-20	all	0-15	16-20	all
LwF-MC [15]	67.2	41.2	60.7	4.5	7.0	5.2
ILT [24]	63.2	39.5	57.3	3.7	5.7	4.2
SDR [61]	74.6	44.1	67.3	59.4	14.3	48.7
PLOP [26]	71.0	42.8	64.3	57.9	13.7	46.5
RCIL [30]	75.0	42.8	67.3	66.1	18.2	54.7
MiB [25]	46.2	12.9	37.9	71.8	43.3	64.7
+ Ours	71.2	31.6	61.8	74.3	45.3	67.4
SSUL [27]	74.0	32.2	64.0	76.4	45.6	69.1
+ Ours	75.2	37.2	66.2	77.4	49.4	70.7
MicroSeg [23]	73.7	24.1	61.9	77.4	43.4	69.3
+ Ours	75.6	26.6	63.9	78.3	46.9	70.9
MicroSeg-M [23]	80.0	<b>47.6</b>	72.3	80.7	55.2	74.7
+ Ours	<b>80.8</b>	46.5	<b>72.6</b>	<b>81.5</b>	<b>60.0</b>	<b>76.4</b>

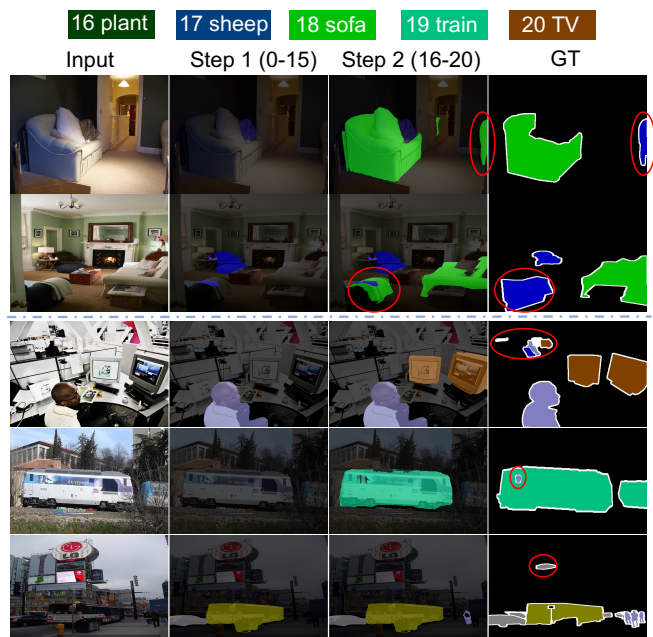


Fig. 7. Failure cases on PASCAL VOC 2012 (15-5 (2 steps)). Method: *MicroSeg+Ours*. Zoom in for details.

segmentation models. We will design specialized architectures to focus on this problem.

## V. LIMITATION

We acknowledge that there are multiple ways to design the feature aggregation module, and this work only explores a few possibilities. Future research can explore more advanced architectures to build upon the insights gained from this work.

## VI. CONCLUSION

To our knowledge, this study is the first to explore the efficient multi-grained knowledge reuse by aggregating multi-level feature when freezing the heavy backbone for class incremental semantic segmentation (CISS). Specifically, we first propose a naïve feature pyramid module and apply it to the

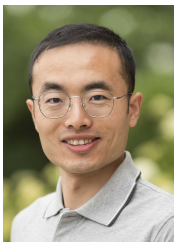
current SOTA method with significant performance gains. Furthermore, a novel densely-interactive feature pyramid (DEFY) is introduced for a better multi-level feature fusion. The advantage of DEFY lies in its ability to establish per-pixel relationships between pairs of features and facilitate dense feature interaction. Moreover, we demonstrate the proposed DEFY can be easily integrated into three representative existing CISS models as a plug-in to enhance their performance. Especially, equipping the current SOTA method with DEFY results in a new state-of-the-art performance.

## REFERENCES

- [1] J. Long, E. Shelhamer, and T. Darrell, "Fully convolutional networks for semantic segmentation," in *Proceedings of the IEEE/CVF Conference on Computer Vision and Pattern Recognition*, 2015, pp. 3431–3440.
- [2] H. Zhao, J. Shi, X. Qi, X. Wang, and J. Jia, "Pyramid scene parsing network," in *Proceedings of the IEEE/CVF Conference on Computer Vision and Pattern Recognition*, 2017, pp. 2881–2890.
- [3] L.-C. Chen, Y. Zhu, G. Papandreou, F. Schroff, and H. Adam, "Encoder-decoder with atrous separable convolution for semantic image segmentation," in *European Conference on Computer Vision*, 2018, pp. 801–818.
- [4] L.-C. Chen, G. Papandreou, I. Kokkinos, K. Murphy, and A. L. Yuille, "DeepLab: Semantic image segmentation with deep convolutional nets, atrous convolution, and fully connected crfs," *IEEE Transactions on Pattern Analysis and Machine Intelligence*, vol. 40, no. 4, pp. 834–848, 2017.
- [5] L.-C. Chen, G. Papandreou, F. Schroff, and H. Adam, "Rethinking atrous convolution for semantic image segmentation," *arXiv preprint arXiv:1706.05587*, 2017.
- [6] J. Fu, J. Liu, H. Tian, Y. Li, Y. Bao, Z. Fang, and H. Lu, "Dual attention network for scene segmentation," in *Proceedings of the IEEE/CVF Conference on Computer Vision and Pattern Recognition*, 2019, pp. 3146–3154.
- [7] Z. Huang, X. Wang, L. Huang, C. Huang, Y. Wei, and W. Liu, "Ccnet: Criss-cross attention for semantic segmentation," in *Proceedings of the IEEE/CVF International Conference on Computer Vision*, 2019, pp. 603–612.
- [8] X. Wang, R. Girshick, A. Gupta, and K. He, "Non-local neural networks," in *Proceedings of the IEEE/CVF Conference on Computer Vision and Pattern Recognition*, 2018, pp. 7794–7803.
- [9] Y. Yuan, L. Huang, J. Guo, C. Zhang, X. Chen, and J. Wang, "Ocnnet: Object context for semantic segmentation," *International Journal of Computer Vision*, vol. 129, no. 8, pp. 2375–2398, 2021.
- [10] R. Strudel, R. Garcia, I. Laptev, and C. Schmid, "Segformer: Transformer for semantic segmentation," in *Proceedings of the IEEE/CVF International Conference on Computer Vision*, 2021, pp. 7262–7272.
- [11] S. Zheng, J. Lu, H. Zhao, X. Zhu, Z. Luo, Y. Wang, Y. Fu, J. Feng, T. Xiang, P. H. Torr *et al.*, "Rethinking semantic segmentation from a sequence-to-sequence perspective with transformers," in *Proceedings of the IEEE/CVF Conference on Computer Vision and Pattern Recognition*, 2021, pp. 6881–6890.
- [12] G. Cauwenberghs and T. Poggio, "Incremental and decremental support vector machine learning," *Advances in Neural Information Processing Systems*, vol. 13, 2000.
- [13] M. McCloskey and N. J. Cohen, "Catastrophic interference in connectionist networks: The sequential learning problem," in *Psychology of learning and motivation*. Elsevier, 1989, vol. 24, pp. 109–165.
- [14] R. Polikar, L. Upda, S. S. Upda, and V. Honavar, "Learn++: An incremental learning algorithm for supervised neural networks," *IEEE Transactions on Systems, Man, and Cybernetics*, vol. 31, no. 4, pp. 497–508, 2001.
- [15] Z. Li and D. Hoiem, "Learning without forgetting," *IEEE Transactions on Pattern Analysis and Machine Intelligence*, vol. 40, no. 12, pp. 2935–2947, 2017.
- [16] G. Hinton, O. Vinyals, J. Dean *et al.*, "Distilling the knowledge in a neural network," *arXiv preprint arXiv:1503.02531*, 2015.
- [17] R. Aljundi, P. Chakravarthy, and T. Tuytelaars, "Expert gate: Lifelong learning with a network of experts," in *Proceedings of the IEEE/CVF Conference on Computer Vision and Pattern Recognition*, 2017, pp. 3366–3375.
- [18] A. Mallya and S. Lazebnik, "Packnet: Adding multiple tasks to a single network by iterative pruning," in *Proceedings of the IEEE/CVF Conference on Computer Vision and Pattern Recognition*, 2018, pp. 7765–7773.
- [19] J. Bang, H. Kim, Y. Yoo, J.-W. Ha, and J. Choi, "Rainbow memory: Continual learning with a memory of diverse samples," in *Proceedings of the IEEE/CVF Conference on Computer Vision and Pattern Recognition*, 2021, pp. 8218–8227.
- [20] E. Belouadah and A. Popescu, "I12m: Class incremental learning with dual memory," in *Proceedings of the IEEE/CVF International Conference on Computer Vision*, 2019, pp. 583–592.
- [21] A. Chaudhry, A. Gordo, P. Dokania, P. Torr, and D. Lopez-Paz, "Using hindsight to anchor past knowledge in continual learning," in *Proceedings of the AAAI Conference on Artificial Intelligence*, vol. 35, no. 8, 2021, pp. 6993–7001.
- [22] C. D. Kim, J. Jeong, S. Moon, and G. Kim, "Continual learning on noisy data streams via self-purified replay," in *Proceedings of the IEEE/CVF International Conference on Computer Vision*, 2021, pp. 537–547.
- [23] Z. Zhang, G. Gao, Z. Fang, J. Jiao, and Y. Wei, "Mining unseen classes via regional objectness: A simple baseline for incremental segmentation," in *Advances in Neural Information Processing Systems*, 2022.
- [24] U. Michieli and P. Zanuttigh, "Incremental learning techniques for semantic segmentation," in *Proceedings of the IEEE/CVF International Conference on Computer Vision Workshops*, 2019, pp. 0–0.
- [25] F. Cermelli, M. Mancini, S. R. Bulò, E. Ricci, and B. Caputo, "Modeling the background for incremental learning in semantic segmentation," in *Proceedings of the IEEE/CVF Conference on Computer Vision and Pattern Recognition*, 2020, pp. 9233–9242.
- [26] A. Douillard, Y. Chen, A. Dapogny, and M. Cord, "Plop: Learning without forgetting for continual semantic segmentation," in *Proceedings of the IEEE/CVF Conference on Computer Vision and Pattern Recognition*, 2021, pp. 4040–4050.
- [27] S. Cha, Y. Yoo, T. Moon *et al.*, "Ssul: Semantic segmentation with unknown label for exemplar-based class-incremental learning," *Advances in Neural Information Processing Systems*, vol. 34, pp. 10919–10930, 2021.
- [28] Q. Hou, M.-M. Cheng, X. Hu, A. Borji, Z. Tu, and P. H. Torr, "Deeply supervised salient object detection with short connections," in *Proceedings of the IEEE/CVF Conference on Computer Vision and Pattern Recognition*, 2017, pp. 3203–3212.
- [29] B. Cheng, I. Misra, A. G. Schwing, A. Kirillov, and R. Girdhar, "Masked-attention mask transformer for universal image segmentation," in *Proceedings of the IEEE/CVF Conference on Computer Vision and Pattern Recognition*, 2022, pp. 1290–1299.
- [30] C.-B. Zhang, J.-W. Xiao, X. Liu, Y.-C. Chen, and M.-M. Cheng, "Representation compensation networks for continual semantic segmentation," in *Proceedings of the IEEE/CVF Conference on Computer Vision and Pattern Recognition*, 2022, pp. 7043–7054.
- [31] K. He, X. Zhang, S. Ren, and J. Sun, "Deep residual learning for image recognition," in *Proceedings of the IEEE/CVF Conference on Computer Vision and Pattern Recognition*, 2016.
- [32] B. Hariharan, P. Arbeláez, R. Girshick, and J. Malik, "Hypercolumns for object segmentation and fine-grained localization," in *Proceedings of the IEEE/CVF Conference on Computer Vision and Pattern Recognition*, 2015, pp. 447–456.
- [33] J. Wang, K. Sun, T. Cheng, B. Jiang, C. Deng, Y. Zhao, D. Liu, Y. Mu, M. Tan, X. Wang *et al.*, "Deep high-resolution representation learning for visual recognition," *IEEE Transactions on Pattern Analysis and Machine Intelligence*, vol. 43, no. 10, pp. 3349–3364, 2020.
- [34] F. Yu and V. Koltun, "Multi-scale context aggregation by dilated convolutions," in *International Conference on Learning Representations*, 2016.
- [35] O. Ronneberger, P. Fischer, and T. Brox, "U-net: Convolutional networks for biomedical image segmentation," in *International Conference on Medical Image Computing and Computer-Assisted Intervention*. Springer, 2015, pp. 234–241.
- [36] B. Cheng, A. Schwing, and A. Kirillov, "Per-pixel classification is not all you need for semantic segmentation," in *Advances in Neural Information Processing Systems*, vol. 34, 2021, pp. 17 864–17 875.
- [37] A. Rosenfeld and J. K. Tsotsos, "Incremental learning through deep adaptation," *IEEE Transactions on Pattern Analysis and Machine Intelligence*, vol. 42, no. 3, pp. 651–663, 2018.
- [38] J. Serra, D. Suris, M. Miron, and A. Karatzoglou, "Overcoming catastrophic forgetting with hard attention to the task," in *International Conference on Machine Learning*. PMLR, 2018, pp. 4548–4557.

- [39] M. De Lange and T. Tuytelaars, "Continual prototype evolution: Learning online from non-stationary data streams," in *Proceedings of the IEEE/CVF International Conference on Computer Vision*, 2021, pp. 8250–8259.
- [40] D. Lopez-Paz and M. Ranzato, "Gradient episodic memory for continual learning," in *Advances in Neural Information Processing Systems*, vol. 30, 2017.
- [41] S.-A. Rebuffi, A. Kolesnikov, G. Sperl, and C. H. Lampert, "icarl: Incremental classifier and representation learning," in *Proceedings of the IEEE/CVF Conference on Computer Vision and Pattern Recognition*, 2017, pp. 2001–2010.
- [42] D. Rolnick, A. Ahuja, J. Schwarz, T. Lillicrap, and G. Wayne, "Experience replay for continual learning," in *Advances in Neural Information Processing Systems*, vol. 32, 2019.
- [43] H. Shin, J. K. Lee, J. Kim, and J. Kim, "Continual learning with deep generative replay," in *Advances in Neural Information Processing Systems*, vol. 30, 2017.
- [44] Y. Oh, D. Baek, and B. Ham, "Alife: Adaptive logit regularizer and feature replay for incremental semantic segmentation," in *Advances in Neural Information Processing Systems*, 2022.
- [45] R. Aljundi, F. Babiloni, M. Elhoseiny, M. Rohrbach, and T. Tuytelaars, "Memory aware synapses: Learning what (not) to forget," in *European Conference on Computer Vision*, 2018, pp. 139–154.
- [46] A. Rannen, R. Aljundi, M. B. Blaschko, and T. Tuytelaars, "Encoder based lifelong learning," in *Proceedings of the IEEE/CVF International Conference on Computer Vision*, 2017, pp. 1320–1328.
- [47] D. Baek, Y. Oh, S. Lee, J. Lee, and B. Ham, "Decomposed knowledge distillation for class-incremental semantic segmentation," in *Advances in Neural Information Processing Systems*, 2022.
- [48] A. Chaudhry, P. K. Dokania, T. Ajanthan, and P. H. Torr, "Riemannian walk for incremental learning: Understanding forgetting and intransigence," in *European Conference on Computer Vision*, 2018, pp. 532–547.
- [49] P. Dhar, R. V. Singh, K.-C. Peng, Z. Wu, and R. Chellappa, "Learning without memorizing," in *Proceedings of the IEEE/CVF Conference on Computer Vision and Pattern Recognition*, 2019, pp. 5138–5146.
- [50] A. Douillard, M. Cord, C. Ollion, T. Robert, and E. Valle, "Podnet: Pooled outputs distillation for small-tasks incremental learning," in *European Conference on Computer Vision*. Springer, 2020, pp. 86–102.
- [51] C. Simon, P. Koniusz, and M. Harandi, "On learning the geodesic path for incremental learning," in *Proceedings of the IEEE/CVF Conference on Computer Vision and Pattern Recognition*, 2021, pp. 1591–1600.
- [52] J. Kirkpatrick, R. Pascanu, N. Rabinowitz, J. Veness, G. Desjardins, A. A. Rusu, K. Milan, J. Quan, T. Ramalho, A. Grabska-Barwinska et al., "Overcoming catastrophic forgetting in neural networks," *Proceedings of the National Academy of Sciences*, vol. 114, no. 13, pp. 3521–3526, 2017.
- [53] A. Iscen, J. Zhang, S. Lazebnik, and C. Schmid, "Memory-efficient incremental learning through feature adaptation," in *European Conference on Computer Vision*. Springer, 2020, pp. 699–715.
- [54] Y. Liu, S. Parisot, G. Slabaugh, X. Jia, A. Leonardis, and T. Tuytelaars, "More classifiers, less forgetting: A generic multi-classifier paradigm for incremental learning," in *European Conference on Computer Vision*. Springer, 2020, pp. 699–716.
- [55] P. Pan, S. Swaroop, A. Immer, R. Eschenhagen, R. Turner, and M. E. E. Khan, "Continual deep learning by functional regularisation of memorable past," *Advances in Neural Information Processing Systems*, vol. 33, pp. 4453–4464, 2020.
- [56] D. Park, S. Hong, B. Han, and K. M. Lee, "Continual learning by asymmetric loss approximation with single-side overestimation," in *Proceedings of the IEEE/CVF International Conference on Computer Vision*, 2019, pp. 3335–3344.
- [57] X. Tao, X. Chang, X. Hong, X. Wei, and Y. Gong, "Topology-preserving class-incremental learning," in *European Conference on Computer Vision*. Springer, 2020, pp. 254–270.
- [58] L. Yu, B. Twardowski, X. Liu, L. Herranz, K. Wang, Y. Cheng, S. Jui, and J. v. d. Weijer, "Semantic drift compensation for class-incremental learning," in *Proceedings of the IEEE/CVF Conference on Computer Vision and Pattern Recognition*, 2020, pp. 6982–6991.
- [59] F. Zenke, B. Poole, and S. Ganguli, "Continual learning through synaptic intelligence," in *International Conference on Machine Learning*. PMLR, 2017, pp. 3987–3995.
- [60] J. Liu, W. Zhou, X. Li, J. Xu, and Z. Chen, "Liqua: Lifelong blind image quality assessment," *IEEE Transactions on Multimedia*, 2022.
- [61] U. Michieli and P. Zanuttigh, "Continual semantic segmentation via repulsion-attraction of sparse and disentangled latent representations," in *Proceedings of the IEEE/CVF Conference on Computer Vision and Pattern Recognition*, 2021, pp. 1114–1124.
- [62] A. Maracani, U. Michieli, M. Toldo, and P. Zanuttigh, "Recall: Replay-based continual learning in semantic segmentation," in *Proceedings of the IEEE/CVF International Conference on Computer Vision*, 2021, pp. 7026–7035.
- [63] V. Badrinarayanan, A. Kendall, and R. Cipolla, "Segnet: A deep convolutional encoder-decoder architecture for image segmentation," *IEEE Transactions on Pattern Analysis and Machine Intelligence*, vol. 39, no. 12, pp. 2481–2495, 2017.
- [64] C. R. Chen, Q. Fan, and R. Panda, "Crossvit: Cross-attention multi-scale vision transformer for image classification," in *Proceedings of the IEEE/CVF International Conference on Computer Vision*. IEEE, 2021, pp. 347–356.
- [65] L. Chen, Y. Yang, J. Wang, W. Xu, and A. L. Yuille, "Attention to scale: Scale-aware semantic image segmentation," in *Proceedings of the IEEE/CVF Conference on Computer Vision and Pattern Recognition*. IEEE Computer Society, 2016, pp. 3640–3649.
- [66] H. Ding, X. Jiang, B. Shuai, A. Q. Liu, and G. Wang, "Context contrasted feature and gated multi-scale aggregation for scene segmentation," in *Proceedings of the IEEE/CVF Conference on Computer Vision and Pattern Recognition*. Computer Vision Foundation / IEEE Computer Society, 2018, pp. 2393–2402.
- [67] J. Fu, J. Liu, H. Tian, Y. Li, Y. Bao, Z. Fang, and H. Lu, "Dual attention network for scene segmentation," in *Proceedings of the IEEE/CVF Conference on Computer Vision and Pattern Recognition*. Computer Vision Foundation / IEEE, 2019, pp. 3146–3154.
- [68] B. Hariharan, P. A. Arbeláez, R. B. Girshick, and J. Malik, "Hypercolumns for object segmentation and fine-grained localization," in *Proceedings of the IEEE/CVF Conference on Computer Vision and Pattern Recognition*. IEEE Computer Society, 2015, pp. 447–456.
- [69] S. Hong, J. Oh, H. Lee, and B. Han, "Learning transferrable knowledge for semantic segmentation with deep convolutional neural network," in *Proceedings of the IEEE/CVF Conference on Computer Vision and Pattern Recognition*. IEEE Computer Society, 2016, pp. 3204–3212.
- [70] Q. Hou, L. Zhang, M. Cheng, and J. Feng, "Strip pooling: Rethinking spatial pooling for scene parsing," in *Proceedings of the IEEE/CVF Conference on Computer Vision and Pattern Recognition*. Computer Vision Foundation / IEEE, 2020, pp. 4002–4011.
- [71] X. Li, Z. Zhong, J. Wu, Y. Yang, Z. Lin, and H. Liu, "Expectation-maximization attention networks for semantic segmentation," in *Proceedings of the IEEE/CVF International Conference on Computer Vision*. IEEE, 2019, pp. 9166–9175.
- [72] D. Lin, Y. Ji, D. Lischinski, D. Cohen-Or, and H. Huang, "Multi-scale context intertwining for semantic segmentation," in *European Conference on Computer Vision (3)*, ser. Lecture Notes in Computer Science, vol. 11207. Springer, 2018, pp. 622–638.
- [73] G. Lin, A. Milan, C. Shen, and I. D. Reid, "Refinenet: Multi-path refinement networks for high-resolution semantic segmentation," in *Proceedings of the IEEE/CVF Conference on Computer Vision and Pattern Recognition*. IEEE Computer Society, 2017, pp. 5168–5177.
- [74] W. Wang, E. Xie, X. Li, D. Fan, K. Song, D. Liang, T. Lu, P. Luo, and L. Shao, "Pyramid vision transformer: A versatile backbone for dense prediction without convolutions," in *Proceedings of the IEEE/CVF International Conference on Computer Vision*. IEEE, 2021, pp. 548–558.
- [75] Z. Liu, Y. Lin, Y. Cao, H. Hu, Y. Wei, Z. Zhang, S. Lin, and B. Guo, "Swin transformer: Hierarchical vision transformer using shifted windows," in *Proceedings of the IEEE/CVF International Conference on Computer Vision*. IEEE, 2021, pp. 9992–10002.
- [76] R. Strudel, R. G. Pinel, I. Laptev, and C. Schmid, "Segformer: Transformer for semantic segmentation," in *Proceedings of the IEEE/CVF International Conference on Computer Vision*. IEEE, 2021, pp. 7242–7252.
- [77] E. Xie, W. Wang, Z. Yu, A. Anandkumar, J. M. Alvarez, and P. Luo, "Segformer: Simple and efficient design for semantic segmentation with transformers," in *Advances in Neural Information Processing Systems*, 2021, pp. 12077–12090.
- [78] D. Zhang, H. Zhang, J. Tang, M. Wang, X. Hua, and Q. Sun, "Feature pyramid transformer," in *European Conference on Computer Vision (28)*, ser. Lecture Notes in Computer Science, vol. 12373. Springer, 2020, pp. 323–339.
- [79] T. Lin, P. Dollár, R. B. Girshick, K. He, B. Hariharan, and S. J. Belongie, "Feature pyramid networks for object detection," in *Proceedings of the IEEE/CVF Conference on Computer Vision and Pattern Recognition*. IEEE Computer Society, 2017, pp. 936–944.

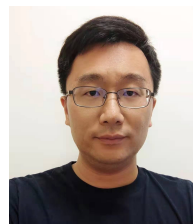
- [80] Z. Xiao, W. Weng, Y. Zhang, and Z. Xiong, "Eva2: Event-assisted video frame interpolation via cross-modal alignment and aggregation," *IEEE Transactions on Computational Imaging*, vol. 8, pp. 1145–1158, 2022.
- [81] X. Li, S. Sun, Z. Zhang, and Z. Chen, "Multi-scale grouped dense network for vvc intra coding," in *Proceedings of the IEEE/CVF Conference on Computer Vision and Pattern Recognition Workshops*, 2020, pp. 158–159.
- [82] B. Li, X. Li, Y. Lu, S. Liu, R. Feng, and Z. Chen, "Hst: Hierarchical swin transformer for compressed image super-resolution," in *European Conference on Computer Vision Workshops*. Springer, 2023, pp. 651–668.
- [83] S. Liu, L. Qi, H. Qin, J. Shi, and J. Jia, "Path aggregation network for instance segmentation," in *Proceedings of the IEEE/CVF Conference on Computer Vision and Pattern Recognition*. Computer Vision Foundation / IEEE Computer Society, 2018, pp. 8759–8768.
- [84] Z. Lu, S. He, X. Zhu, L. Zhang, Y.-Z. Song, and T. Xiang, "Simpler is better: Few-shot semantic segmentation with classifier weight transformer," in *Proceedings of the IEEE/CVF International Conference on Computer Vision*, 2021, pp. 8741–8750.
- [85] Z. Lu, S. He, D. Li, Y.-Z. Song, and T. Xiang, "Prediction calibration for generalized few-shot semantic segmentation," *IEEE Transactions on Image Processing*, 2022.
- [86] M. Everingham, L. Van Gool, C. K. Williams, J. Winn, and A. Zisserman, "The pascal visual object classes (voc) challenge," *International Journal of Computer Vision*, vol. 88, pp. 303–338, 2010.
- [87] B. Zhou, H. Zhao, X. Puig, S. Fidler, A. Barriuso, and A. Torralba, "Scene parsing through ade20k dataset," in *Proceedings of the IEEE/CVF Conference on Computer Vision and Pattern Recognition*, 2017, pp. 633–641.
- [88] J. Deng, W. Dong, R. Socher, L.-J. Li, K. Li, and L. Fei-Fei, "Imagenet: A large-scale hierarchical image database," in *Proceedings of the IEEE/CVF Conference on Computer Vision and Pattern Recognition*, 2009, pp. 248–255.
- [89] T. Liu, Z. Yuan, J. Sun, J. Wang, N. Zheng, X. Tang, and H.-Y. Shum, "Learning to detect a salient object," *IEEE Transactions on Pattern Analysis and Machine Intelligence*, vol. 33, no. 2, pp. 353–367, 2010.
- [90] T.-Y. Lin, M. Maire, S. Belongie, J. Hays, P. Perona, D. Ramanan, P. Dollár, and C. L. Zitnick, "Microsoft coco: Common objects in context," in *European Conference on Computer Vision*. Springer, 2014, pp. 740–755.
- [91] J.-W. Xiao, C.-B. Zhang, J. Feng, X. Liu, J. van de Weijer, and M.-M. Cheng, "Endpoints weight fusion for class incremental semantic segmentation," in *Proceedings of the IEEE/CVF Conference on Computer Vision and Pattern Recognition*, 2023, pp. 7204–7213.



**Zhihe Lu** is now a Research Fellow at National University of Singapore. He received the Ph.D. degree at Centre for Vision, Speech and Signal Processing (CVSSP), University of Surrey in 2022, and the master degree at Chinese Academy of Sciences, Institute of Automation (CASIA) in 2019. His research interest centers around transfer learning, few-shot learning, and continual learning. Recently, he focuses on transferring the knowledge of large-scale foundation models to downstream tasks. His articles have been published in major venues including CVPR, ICCV, ACM MM, and TIP. He regularly serves as a reviewer of TPAMI, IJCV, TIP, CVPR, ICCV, ECCV, NeurIPS, ICML, and AAAI.



**Shuicheng Yan** is visiting Beijing Academy of Artificial Intelligence (non-profit organization), and former Group Chief Scientist of Sea Group. He is a Fellow of Singapore's Academy of Engineering, AAAI, ACM, IEEE, and IAPR. His research areas include computer vision, machine learning, and multimedia analysis. Till now, Prof Yan has published over 600 papers at top international journals and conferences, with an H-index of 130+. He has also been named among the annual World's Highly Cited Researchers eight times. His team received ten-time winners or honorable-mention prizes at two core competitions, Pascal VOC and ImageNet (ILSVRC), deemed the "World Cup" in the computer vision community. Besides, his team won more than ten best papers and best student paper awards, particularly a grand slam at the ACM Multimedia, the top-tiered conference in multimedia, including the Best Paper Awards thrice, Best Student Paper Awards twice, and Best Demo Award once.



**Xinchao Wang** is currently an assistant professor in the Department of Electrical and Computer Engineering, National University of Singapore (NUS). Before joining NUS, he was a tenure-track assistant professor of Computer Science at Stevens Institute of Technology, and a SwissNSF postdoctoral fellow at University of Illinois Urbana-Champaign with Prof. Thomas S. Huang. He received a PhD from Ecole Polytechnique Federale de Lausanne, and a first-class honorable degree from Hong Kong Polytechnic University. His research interests include artificial intelligence, computer vision, machine learning, medical image analysis, and multimedia. His articles have been published in major venues including CVPR, ICCV, ECCV, NeurIPS, ICLR, AAAI, IJCAI, ACL, MICCAI, TPAMI, IJCV, TIP, TKDE, and TMI. He has been or is currently serving as an associate editor of IEEE Transactions on Circuits and Systems for Video Technology, Journal of Visual Communication and Image Representation, and Pattern Recognition. He regularly serves as an area chair of CVPR, ICCV, ECCV, NeurIPS, ICPR, ICIP, ICME, and as a senior program committee member of AAAI and IJCAI. His team has been winner of several international challenging, including NTIRE Super-resolution Challenge'18 and AI City Challenge'17. He received the best editor award of JVCI for 2020.